METHOD OF SPECTRAL COMPENSATION LIKE AN EFFECTIVE TOOL TO REDUCE AN EFFECT OF INTERFERING COMPONENTS ON THE MEASUREMENT OF CO2, CH4, CO, AND SO2 IN ATMOSPHERE

Vitaly V. Beloborodov, PhD
Leonid A. Konopelko, Dr., Prof.

D.I.Mendeleyev Institute for Metrology
19, Moskovsky ave., 198005, St.Petersburg, Russia
Tel.:+7-812-323-9654, Fax: +7-812- 327-9776, E-mail: vvb@b10.vniim.ru

ABSTRACT

Method of spectral compensation is examined for the purposes of remote control of CO2, CH4, CO, and SO2 in atmosphere.

Results of calculations on basis of HITRAN database are presented.

It is shown that for NDIR and NDUV instruments an effect of different interfering species including H2O on the measurement of CO2, CH4, CO, and SO2 in atmosphere at open optical paths can be reduced very strongly.

Besides the effects of light source instabilities, changes in the spectral transfer function of the optics, and changes in the detector's spectral responsivity on the measurement also is minimized.

INTRODUCTION

The efforts of scientists working with the gas-filter correlation (GFC) technique have been intended mostly to remove or diminish the effect that interfering species with linear spectra have on measurement results. The nature of this effect has been analyzed.[1,2] Methods have been proposed to solve the problem when the absorption lines of the interfering absorbers' spectra fall mostly on tops of or overlap absorption lines of the measured component.[3,4] The essence of the known methods is that the interfering species are added to one or to both measuring channels of the GFC instrument, thus compensating for the effect of interfering absorption lines in the spectral radiation that reaches the detector.

In addition changes in the structureless interfering spectrum in the bandpass of the GFC instrument and changes of the curvature of the bandpass or continuum can affect the result of the measurement. It can be a problem to achieve the required accuracy for conventional or remote control in the UV or in the IR when spectra of other absorbers are present.

Our goal in the present paper is to introduce a general method of compensating for the effect of structureless and structured interfering spectra on measurements made by the GFC instrument.

Another goal is to show the result of calculations.

METHOD

The result of multiplication of the light source spectral irradiance $I_{S,\lambda}$, the transmittance of the sample cell $T_{S,\lambda}$ filled with the interfering species, the transfer function of the optics $T_{O,\lambda}$, and the responsivity of the detector $R_{D,\lambda}$ yields for spectral change of $I_{S,\lambda}$ or $T_{S,\lambda}$ or $T_{O,\lambda}$ or $R_{D,\lambda}$ the total change of curvature incline on the output of the detector from $(I_{S,\lambda}T_{S,\lambda}T_{O,\lambda}R_{D,\lambda})^1$ to

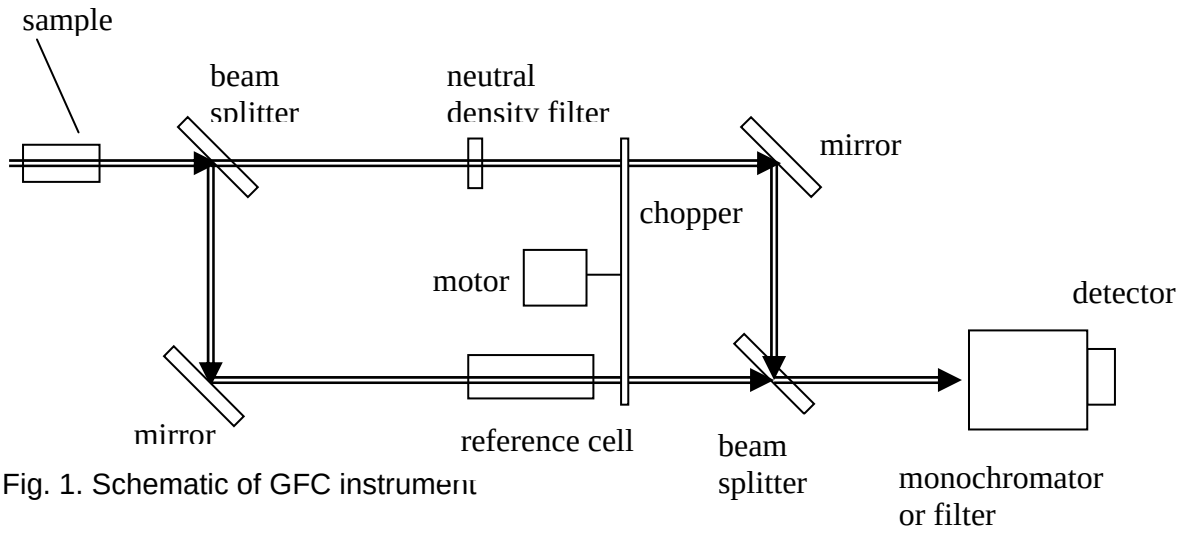

Fig. 1. Schematic of GFC instrument

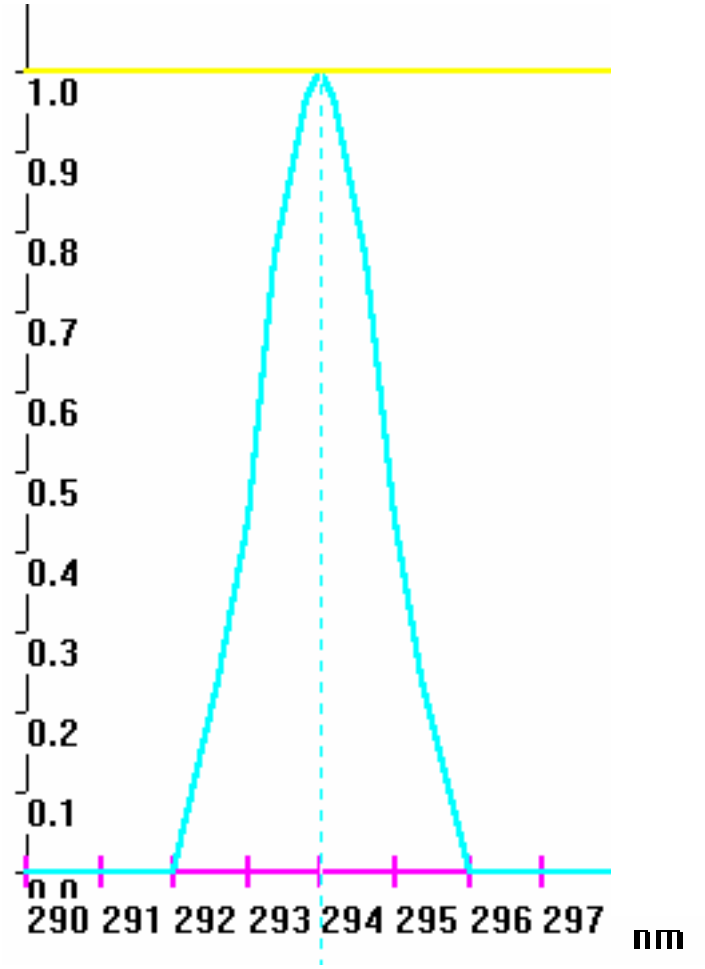

Fig. 2. Bandpass filter profile used for calculations in the UV

$(I_{S,\lambda}T_{S,\lambda}T_{O,\lambda}R_{D,\lambda})^2$. The generic essence of the method of spectral compensation is that the output signal produced by the GFC instrument (with respect to Fig. 1) and expressed as

$$S=\left(\int_{+\infty}^{-\infty} I_{S,\lambda}T_{S,\lambda}T_{N,\lambda}T_{F,\lambda}T_{O,\lambda}R_{D,\lambda}d\lambda - \int_{+\infty}^{-\infty} I_{S,\lambda}T_{S,\lambda}T_{R,\lambda}T_{F,\lambda}T_{O,\lambda}R_{D,\lambda}d\lambda\right) / \int_{+\infty}^{-\infty} I_{S,\lambda}T_{S,\lambda}T_{N,\lambda}T_{F,\lambda}T_{O,\lambda}R_{D,\lambda}d\lambda \quad (1)$$

is zero for structureless spectra for some wavelengths.[5]

Here $T_{N,\lambda}$ - is the transmittance of the neutral density filter; $T_{R,\lambda}$ is the transmittance of the reference cell; $T_{F,\lambda}$ - is the transmittance of the bandpass filter or the transmittance of the monochromator slit. The symbol λ indicates wavelength, and all quantities that have a λ subscript might vary with λ.
Figure 2 shows the bandpass filter profile used in the calculations in the UV with a 2 nm bandwidth at 0.5 peak transmittance Δλ(0.5). The bandpass filter profile is quite realistic but it does not account for out-of-band leakage however.
The monochromator slit profile is triangle.
It means that the interference from the interfering absorbers having structureless spectra is also zero at certain wavelengths.
The bands of integration in practice are extended only over the range where $T_{F,\lambda}$ varies appreciably from zero.
$T_{S,\lambda}$ can be calculated as

$$T_{S,\lambda} = T_{S,I,\lambda}\, T_{S,M,\lambda} \qquad (2)$$

Here $T_{S,I,\lambda}$ is the transmittance of the interfering species in the sample cell; $T_{S,M,\lambda}$ is the transmittance of the measured component in the sample cell.
The use of absorption spectroscopy for the measurement of gas concentrations is based on the Bouguer-Beer-Lambert law of absorption for monochromatic radiation

$$T_{\lambda} = \exp^{-K_{\lambda} CL} \qquad (3)$$

Here K_{λ} is the absorption cross-section of the component at wavelength λ (cm^2); C is the concentration of component assumed homogeneous over the radiation beam (cm^{-3}); and L is the pathlength along the line of propagation in the sample cell (cm).
The integral content of the measured gas on the pathlength L is designated as $w_m = C_m L$ and the integral content of interfering species as $w_i = C_i L$.
IR spectrum of H2O being the main interfering absorber in the IR is strongly structured meanwhile.
The method of spectral compensation effectively works in the case of the interfering species having structured spectra as well if the convolution of $(I_{S,\lambda} T_{S,I,\lambda} T_{O,\lambda} R_{D,\lambda})$ and $T_{F,\lambda}$ is relatively structureless which means that the optical filter or the monochromator slit bandwidth at 0.5 peak transmittance Δλ(0.5) has to be rather high comparing to the spectral shift between the lines of the interfering absorber. The received convolution structure and its incline depend on the structure of the interfering species spectra and the spectral width of the monochromator slit or the bandpass filter.
The achieved with the use of the appropriate spectral bandwidth of the monochromator slit or optical filter Δλ(0.5) structureless convolution $\bar{T}_{I,\lambda_0}$ of the structured transmittance of the interfering species makes similar influence on the measurements as do the structureless functions due to the presence of interfering absorbers or light source instabilities, changes in the spectral transfer function of the optics, and changes in the detector's spectral responsivity.[5]

The simplified normalized convolution $\overline{T}_{N,I,\lambda_0}$ curves depending on the spectral change of $I_{S,\lambda}$ or $T_{S,\lambda}$ or $T_{O,\lambda}$ or $R_{D,\lambda}$ and changing its curvature incline from $\overline{T}_{N,I,\lambda_0}{}^{1}$ to $\overline{T}_{N,I,\lambda_0}{}^{2}$ are shown in Fig. 2a (Here we primarily look at the transmittance of the interfering species in the sample cell). For the sake of simplicity, let's assume that the transmittance of the bandpass filter $T_{F,\lambda}$ is unity from wavelength λ_1 to λ_5, and is zero elsewhere (Fig. 2b). λ_0 is the central wavelength of the bandpass filter or the monochromator slit in this paper.
A simplified transmission spectrum of the gas in the reference cell is illustrated in Fig. 2c. λ_3 is the peak transmittance wavelength of the line-shaped function of the component in the reference cell. λ_2 is the wavelength of sharp transition from perfect transmittance to 0.33 transmittance and λ_4 is the wavelength of sharp transition from 0.33 transmittance to perfect transmittance. The transmittance in the wavelength range from λ_2 to λ_4 is unity. We added here (comparing Fig. 3 in

Reference 5) one line of the measured component to the left from the line-shaped function in the center and another line of the measured component to the right just to simulate the structured spectrum of the absorbers in the IR.

The results of multiplication of curves shown in Figs. 3a and 3c ($T_{F,\lambda}$ shown in Fig. 3b is a part of the calculation of the convolution) for λ_0 near λ_3 are presented in Figs. 3d and 3e. It is obvious that the area under the curve shown in Fig. 3d is equal the area under the curve shown in Fig. 3e, because the decrease of the area for λ_1 to λ_3 shown in Fig. 3e due to the change of the curvature incline from $\overline{T}_{N,I,\lambda_0}{}^{1}$ to $\overline{T}_{N,I,\lambda_0}{}^{2}$ is adequate of its increase for λ_3 to λ_5. So, the detector output signal proportional to the quantity of radiation transmitted through the sample cell and the reference cell will not change in this case. (The detector output signal proportional to the quantity of radiation transmitted through the sample cell and the neutral cell will not change in any case). At the same time the results of multiplication of curves shown in Figs. 3a and 3c will not be equal if we shift the central wavelength of the bandpass filter λ_0 to λ_2 or λ_4. This effect for one line-shaped function of the measured component was described previously.[5] It is obvious that in reality when there are lines with different profiles and intensities the balance has to be found with the help of optimization procedures tuning the central wavelength of the bandpass filter or the monochromator slit λ_0 and its spectral bandwidth $\Delta\lambda(0.5)$.

In a real instrument, compensation for changes in interfering spectra can be achieved by inserting and removing an additional optical filter of any needed nature with the appropriate characteristics along the light path of the gas analyzer to modulate the spectral change, and by shifting the central wavelength of the bandpath filter.[6]

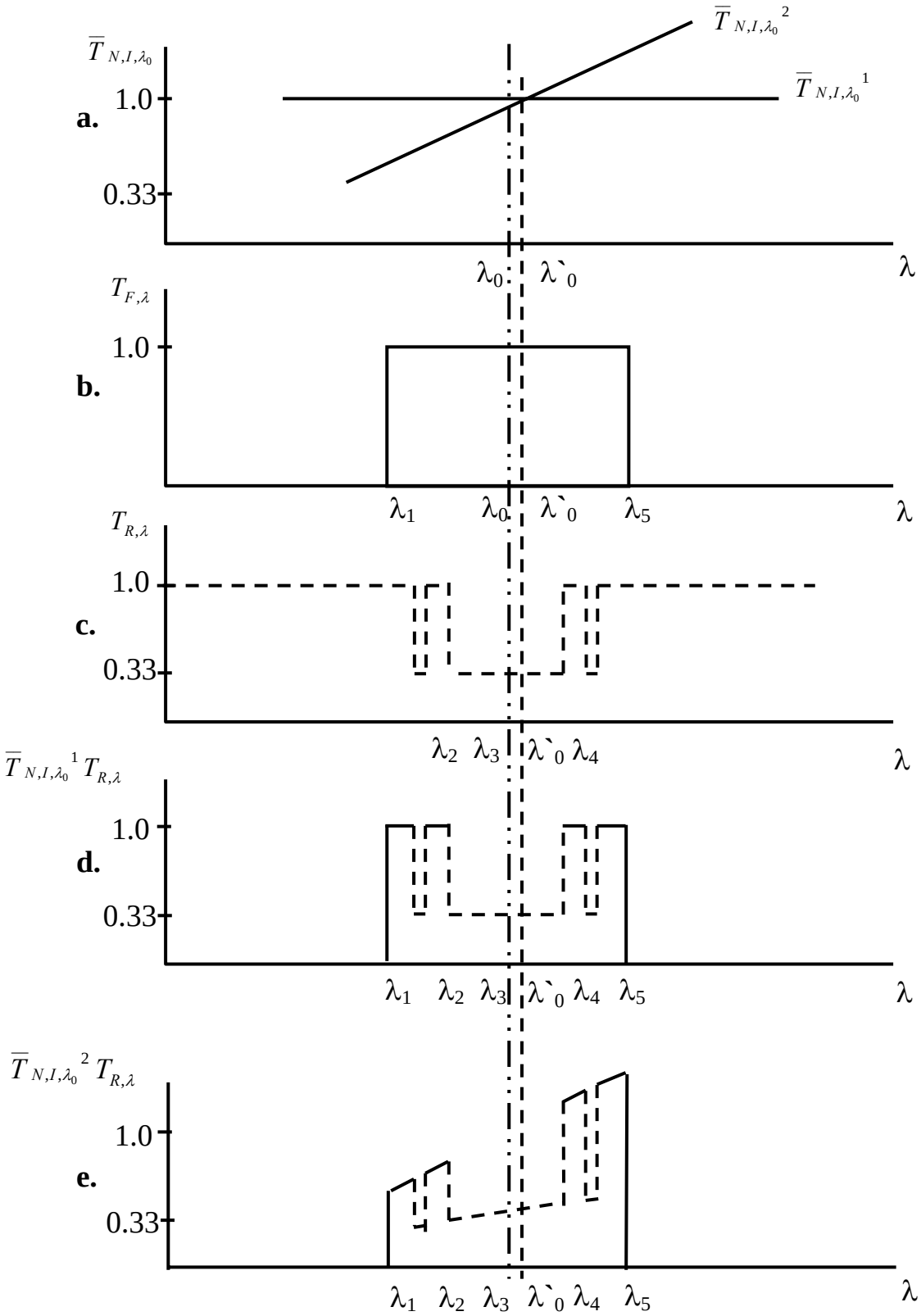

Fig. 3. Method of spectral compensation in the infrared.

COMPLEX COMPUTATION SOFTWARE 'COMPCOM'

CompCom is a Windows based computer program written primarily to simulate the optical gas analyzers performance.
The first stage of such simulation is the generation of spectra and convolution. The spectra can be used as reference spectra for different monitoring applications including conventional, in-situ or remote methods of control of gaseous substances.
The second stage of the gas analyzers performance simulation is the generation of the results showing the sensitivity, zero and span drift of the chosen gas analyzer.
CompCom utilizes its own UV database (program subpart CompCom_UVDB) with more than 120 substances and the HITRAN database of fundamental spectral line parameters[7] to generate transmittance or absorbance spectra for the first stage of simulation for various conditions of temperature, pressure, path length, gas concentrations, spectral resolution, and apodization.

RESULTS

The NDUV and NDIR versions of the software, "CompCom," for complex computations of the optical gas analyzers characteristics has been used in this work. All calculations were made for atmospheric pressure and 296 °K temperature. For simplicity the light source spectral irradiance $I_{S,\lambda}$, the spectral transfer function of the optics $T_{O,\lambda}$ and the spectral responsivity of the detector $R_{D,\lambda}$ are chosen to be unity in the 290 to 310 nm spectral range to measure SO_2 in the presence of O_3 as the interfering absorber. These parameters are also chosen to be unity to measure CO and CO_2 in the presence of H_2O in the 2075 – 2225 cm^{-1} and in the 2275 – 2425 cm^{-1} spectral range correspondently.
Calculations for SO_2 as the measured component in UV were made with the 0.2 nm consecutive shift of the central wavelength of the bandpass filter from 294 to 306 nm.
Calculations for CO and CO_2 as the measured substances were made with the 0.01 cm^{-1} consecutive shift of the central wavelength of the monochromator slit. The first isotope lines only were taken into consideration for calculations in IR. The "line by line" method was implemented for calculations of the Lorentz profile of lines taking into account the dependence of the lines spectral half-width and the lines intensities from the temperature and pressure and taking into account the effect of self-broadening.
The integral content of SO_2, CO or CO_2 in the reference cell was assumed to be w_r = 1000 ppm m (parts per million times path-length).
The curve illustrating the signal output as a function of the wavelength for 500 ppm m of SO_2 in the sample cell in the absence of any interfering absorbers for $\Delta\lambda(0.5)$ = 2 nm is presented in Fig. 4a. It has to be noticed that there are no UV spectra in the 290 – 310 nm spectral range of H_2S, CO or H_2O, which are designated by U.S.EPA[8] as the interfering absorbers for the ambient control of SO_2. But for remote control or control on open optical paths of SO_2 emissions O_3 is the very important interfering absorber. The absorption cross-sections of SO_2 and O_3 and the

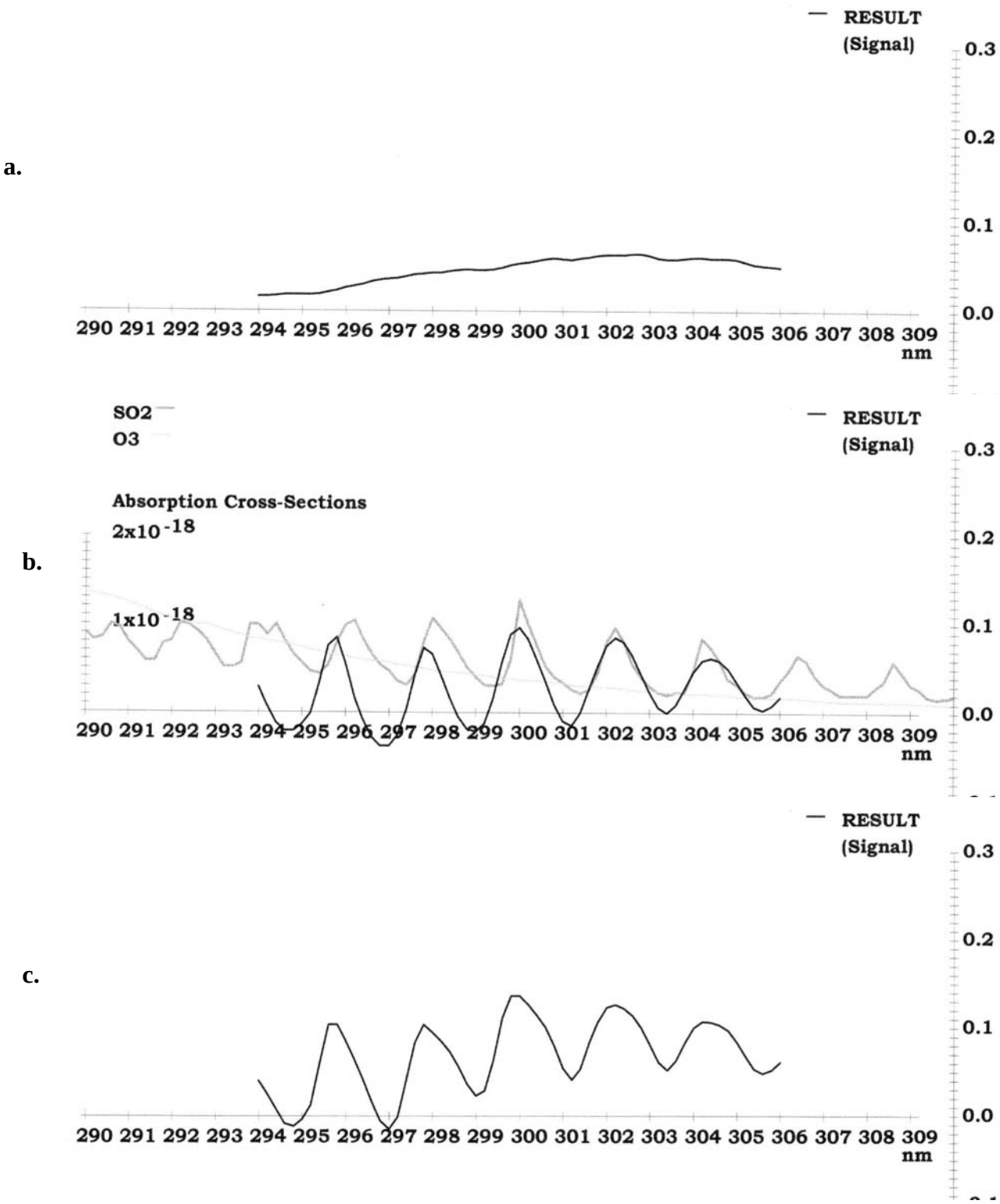

Fig. 4. SO_2 GFC instrument. O_3 interference. a, Curve illustrating the signal output for w_m = 500 ppm m of SO_2 in the sample cell in the absence of any interfering absorbers for $\Delta\lambda(0.5)$ = 2 nm and w_r = 1000 ppm m. b, Absorption cross sections of SO_2 and O_3 (square centimeters) and signal; w_r = 1000 ppm m, w_{i1} = 0, w_{i2} = 10,000 ppm m, w_m = 0, $\Delta\lambda(0.5)$ = 2 nm. c, Signal; w_r = 1000 ppm m, w_{i1} = 0, w_{i2} = 10,000 ppm m, w_m = 500 ppm m, $\Delta\lambda(0.5)$ = 2 nm.

result of calculations of the interference of O_3 in relative units are presented in Fig. 4b. In the cases of O_3 as interfering absorber there are points where the interference curve crosses the abscissa – points where there are no O_3 interference. The value of the signal output for 500 ppm m of SO_2 in the sample cell in absence of the other interfering absorbers (Fig. 4a) shows that the interference of O_3 can be substantial (Fig. 4b). Figure 4b illustrates the zero drift. The span drift has to be studied also especially for the points where the curve intersects at the zero signal point in the absence of the measured gas which is SO_2 for our calculations. Figure 4c illustrates the signal output as a function of the wavelength for 500 ppm m of SO_2 in the sample cell in the case of O_3 integral content change from 0 to 10,000 ppm m for $\Delta\lambda(0.5)$=2 nm. Analyzing Figures 4a, 4b and 4c we can see that in some points of the signal intersection with the abscissa in the absence of SO_2 in the sample cell (Fig. 4b) there are the points of intersection at which the signal output in the presence of SO_2 and in the presence of O_3 in the sample cell (Fig. 4c) does not differ much from the value of the signal output in the presence of SO_2 and in the absence of O_3 as the interfering absorber (Fig. 4a) at the same wavelength – the span drift is minimal. The span drift that is due to O_3 interference for majority of the points of intersection is within required by the U.S.EPA[9] 7% of the interference influence.

The same effects we can see in the IR.

The curves illustrating the spectra, the convolution and the signal output as a function of the wavelength for 5 ppm m of CO in the sample cell in the absence of any interfering absorbers in relative units in the 2075 – 2225 cm^{-1} spectral range are presented in Fig. 5a. The spectra, the normalized convolution for the interfering absorber (i.e. H_2O) and the result of calculations of the interference of H_2O in the absence of CO in relative units as a function of the wavelength are presented in Fig. 5b. (The spectrum of the interfering absorber and the convolution are calculated for w_{i2}). The values of the signal output for 5 ppm m CO in the sample cell in absence of the interfering absorbers (Figs. 5a) show the level of H_2O interference presented on Fig. 5b. The result of calculations shown on Fig. 5b –illustrates the zero drift. Figure 5c illustrates the span drift for 5 ppm m of CO in the sample cell in the case of H_2O integral content change from 300,000 to 400,000 ppm m.

Analyzing Figs. 5a, 5b and 5c for establishing the span drift from H_2O interference we can see that at practically all points of the signal intersection with the abscissa in the absence of CO in the sample cell (Fig. 5b) the signal output with CO and H_2O in the sample cell (Fig. 5c) does not differ much from the value of the signal output with CO and no H_2O (Fig. 5a) at the same wavelength. The span drift that is due to H_2O interference for all points of intersection is within required by the U.S.EPA 7 ppm (in the case of 1 m sample cell path length) of the interference influence in spite of 10% of H_2O content change (from 300,000 to 400,000 ppm m) and instead of 3.5% recommended limit of H_2O[9].

We see the same effects for CO_2 as the measured component and H_2O as the interfering absorber in the 2275 – 2425 cm^{-1} spectral range (Figs. 6a – 6c). The span drift is within required by the U.S.EPA [9] 7% and within required by the WMO[10] 0.05 ppm (in the case of 1 m sample cell path length) in spite of 10% of H_2O content change (from 0 to 100,000 ppm m) instead of 3% H_2O volume permitted by the WMO[10].

The values of the signal output for 5 ppm m of CH_4 in the sample cell in absence of the interfering absorbers (Fig. 7a) show the level of interference presented on Figs. 7b and 7c.

Figures 7b and 7c illustrate the zero drift of CH_4 instrument, which is negligible for many points. The span drift of CH_4 GFC analyzer due to the H_2O interfering species is assumed negligible also for the chosen for calculations contents and so is not illustrated. (The difference in CH_4 and H_2O signals is about two orders, Figs. 7a – 7c).

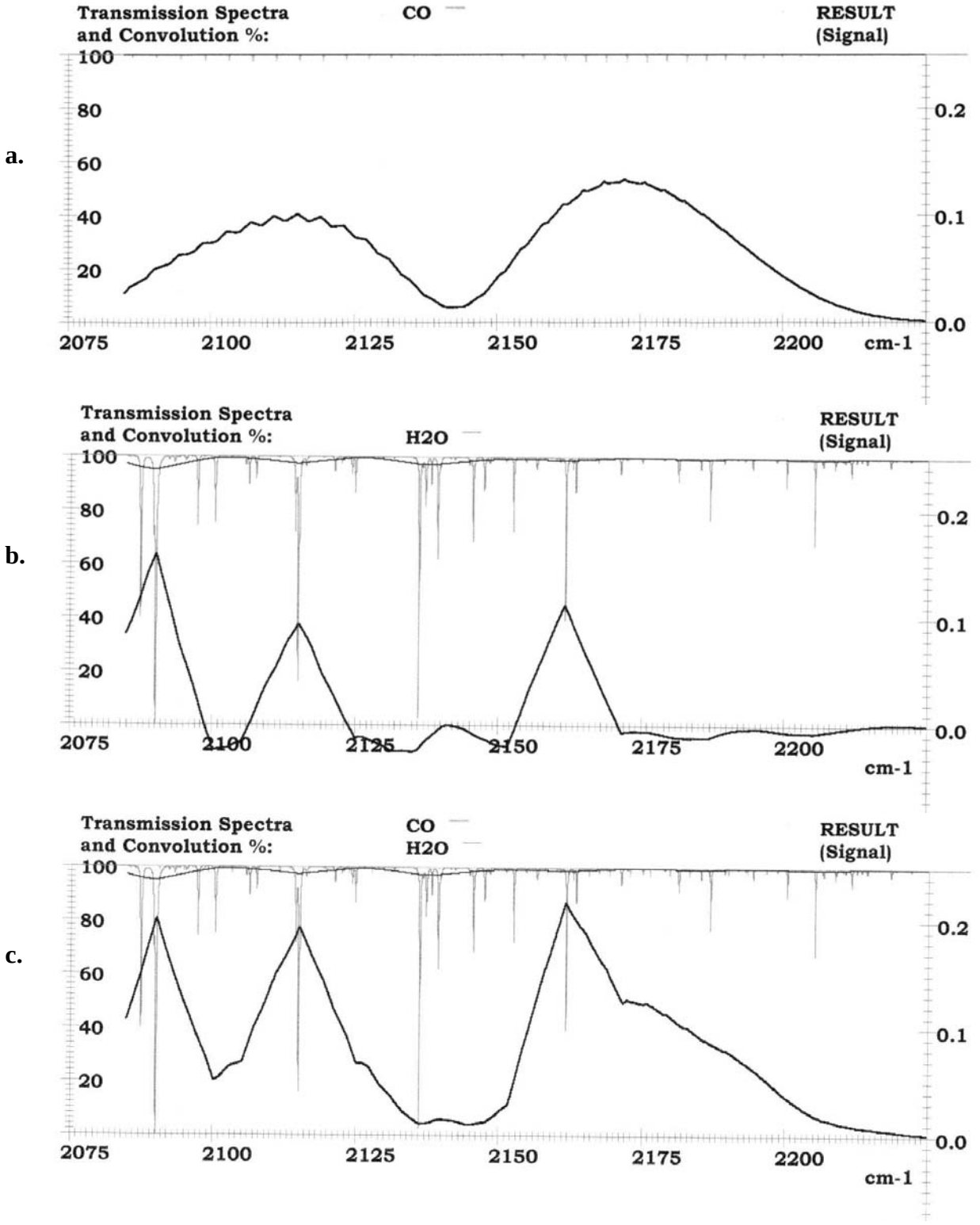

Fig. 5. CO GFC instrument. H_2O interference. Transmission spectra, convolution and signal.
a, Curve illustrating output for w_m = 5 ppm m of CO in the sample cell in the absence of any interfering absorbers for $\Delta\lambda(0.5)$ = 10 cm^{-1} and w_r = 1000 ppm m. b, Curve illustrating output for w_r = 1000 ppm m, w_{i1} = 300,000 ppm m, w_{i2} = 400,000 ppm m, w_m = 0, $\Delta\lambda(0.5)$ = 10 cm^{-1}.
c, Curve illustrating output for w_r = 1000 ppm m, w_{i1} = 300,000 ppm m, w_{i2} = 400,000 ppm m, w_m = 5 ppm m, $\Delta\lambda(0.5)$ = 10 cm^{-1}. Curve illustrating output for

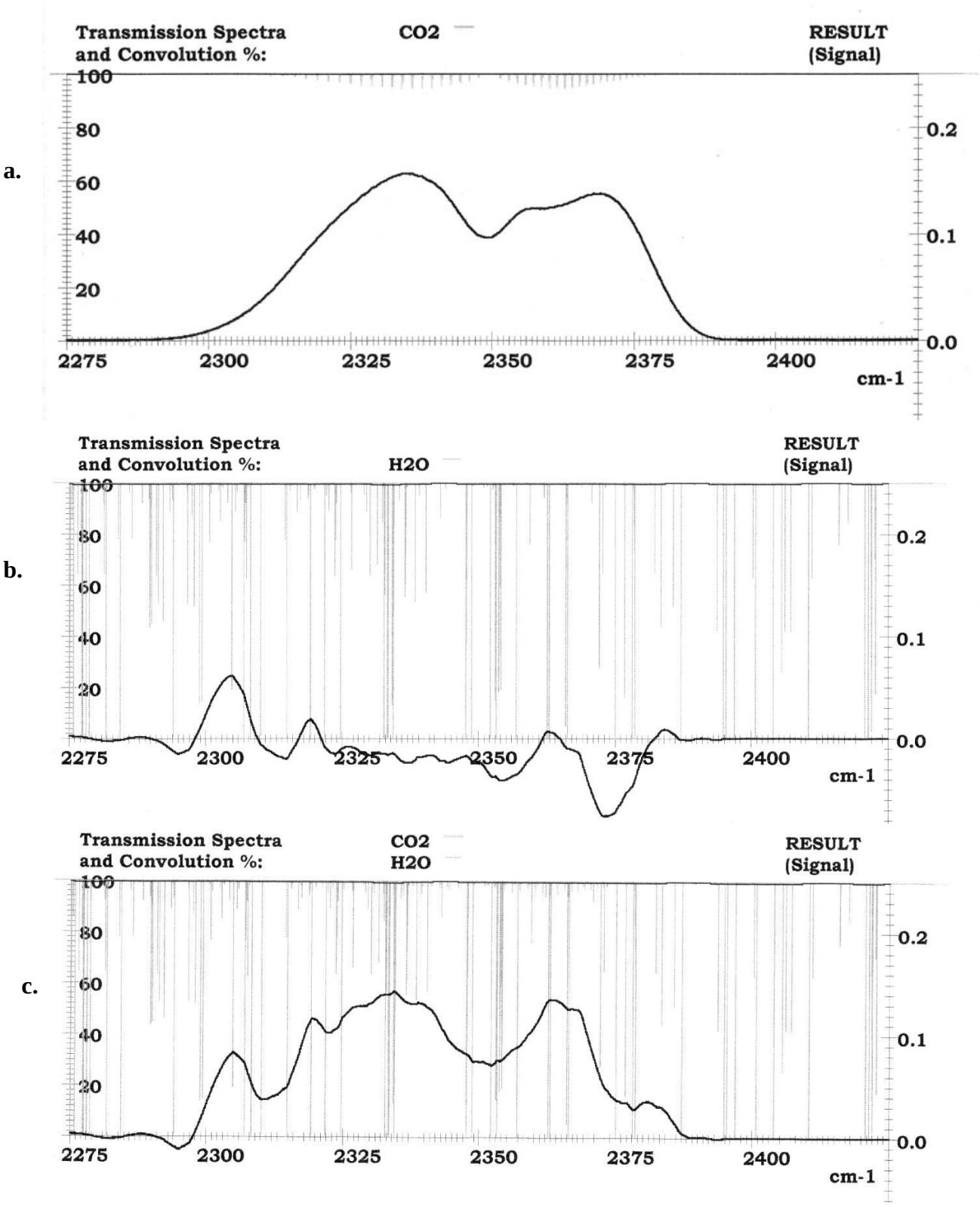

Fig. 6. CO_2 GFC instrument. H_2O interference. Transmission spectra, convolution and signal. a, Curve illustrating output for w_m = 1 ppm m of CO_2 in the sample cell in the absence of any interfering absorbers for $\Delta\lambda(0.5)$ = 10 cm^{-1} and w_r = 1000 ppm m. b, Curve illustrating output for w_r = 1000 ppm m, w_{i1} = 0, w_{i2} = 100,000 ppm m, w_m = 0, $\Delta\lambda(0.5)$ = 10 cm^{-1}.
c, Curve illustrating output for w_r = 1000 ppm m, w_{i1} = 0, w_{i2} = 100,000 ppm m, w_m = 1 ppm m, $\Delta\lambda(0.5)$ = 10 cm^{-1}.

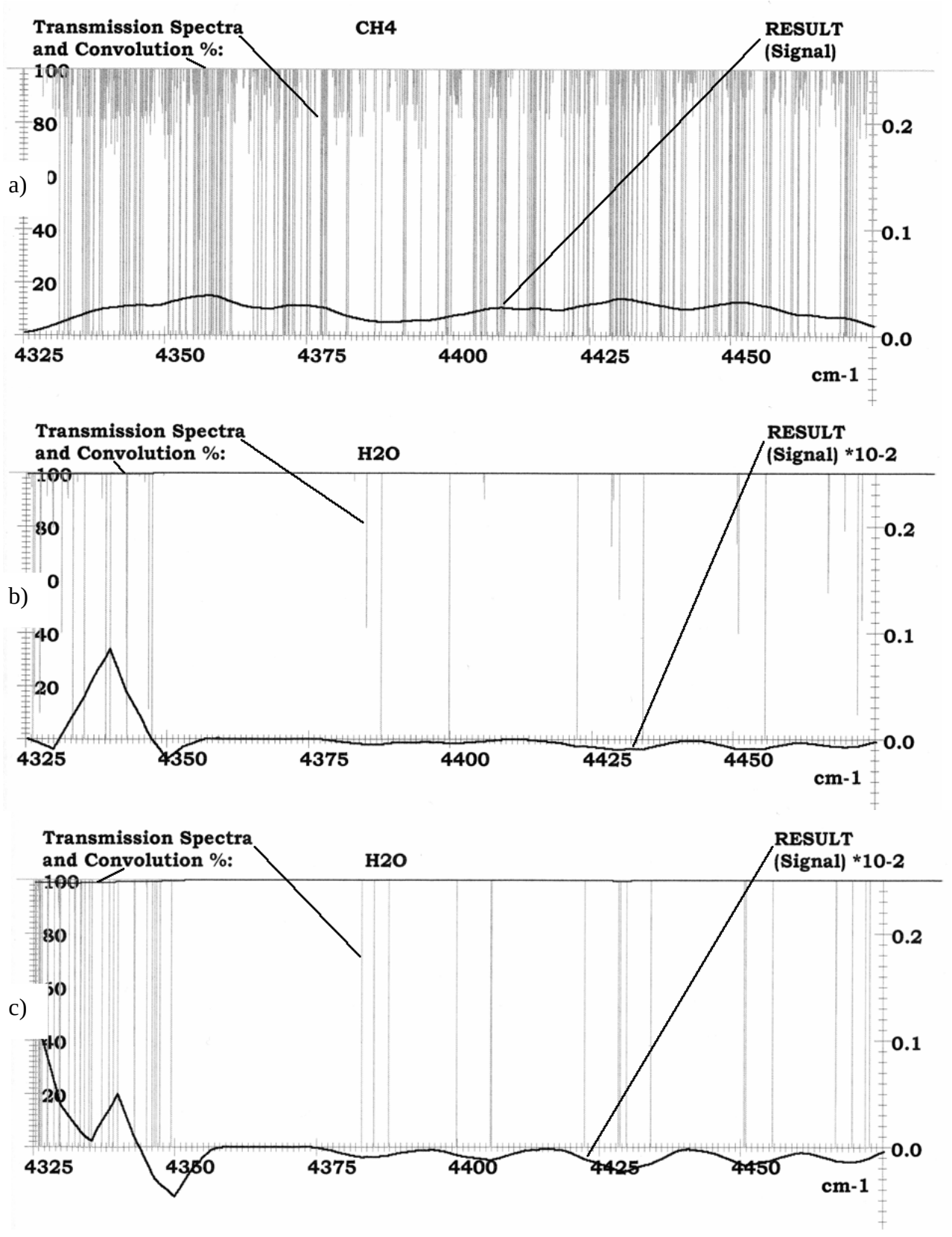

Fig. 7. H_2O interference. (CH_4 GFC instrument).

a, Curve illustrating the signal output of the CH_4 GFC instrument for w_m=5 ppm m of CH_4 in the sample cell in the absence of any interfering absorbers for $\Delta\lambda$ (0,5)=10 cm^{-1} and w_r=1000 ppm m.

b, Small range H_2O interference. w_r=1000 ppm m, w_m=0, w_{i1}=0 ppm m, w_{i2}=1000 ppm m, $\Delta\lambda$(0,5)=10 cm^{-1}.

c, Big range H_2O interference. w_r=1000 ppm m, w_m=0, w_{i1}=0, w_{i2}=1000,000,000 ppm m, $\Delta\lambda$(0,5)=10 cm^{-1}.

CONCLUSION

Our goal in the present paper is to introduce a general method of compensating for the effect of spectra changes that are due to the presence of interfering absorbers or light source instabilities, changes in the spectral transfer function of the optics, and changes in the detector's spectral responsivity. Illustration of the possibilities of the introduced method to be used for SO_2 control in the UV in presence of O_3 and CO or CO_2 control in the IR in presence of H_2O was another goal. Figure 3 illustrates the essence of the method and Figs. 4 to 6 show that the introduced method does reduce the interference from O_3 for SO_2 control in the UV and from H_2O for CO and CO_2 control in the IR. It is shown that there are the wavelengths in the spectrum where the effect of the interfering species on the result of measurement can be drastically reduced and where the span drift is small. The bandwidth of the bandpass filter has to be adjusted to minimize the effect of the interfering species, light source instability, changes in the spectral transfer function of the optics, and changes in the detector's spectral responsivity.
The distinction of the introduced method is in reducing the effect of changes of any kind of the interfering spectra on the measurement performed by the GFC technique whatever the cause of such changes is.

REFERENCES

1. D.E.Burch and D.A.Gryvnak, "Cross-stack measurement of pollutant concentrations using gas-cell correlation spectroscopy" in *Analytical Methods Applied to Air Pollution Measurements,* R.K.Stevens, ed (Ann Arbor Science, 1974) pp. 193 – 231.
2. J.Laurent, "Radiometre a modulation selective pour la detection a distance de pollutants gazeax", Mesures, Regulation, Automatisme, # 7, 39-46 (1977), in French.
3. W.J.Baker, "Systematic approaches to continuous infrared analyzes sensitization", Anal. Chem., Vol. 28, # 9, 1391-1396 (1954).
4. O.G.Koppius, "Analysis of mixtures with double-beam nondispersive infrared instrument", Anal. Chem., Vol. 23, # 4, 554-559 (1951).
5. Beloborodov V.V. "Method of sectral compensation and its application in the ultraviolet for sulfur dioxide control with a gas-filter correlation instrument", Appl. Opt., 2002, Vol. 41, # 18, 3517-3522.
6. Beloborodov V.V.; Reshetnikov A.I. "Correlation radiometer", Russian patent # 1533490, Application # 4335374, Priority: November 30, 1987, Registered: January 27, 1993.
7. Rothman, L.S. et al. "The HITRAN Molecular Spectroscopic Database and Hawks (HITRAN Atmospheric Workstation): 1996 Edition", J. Quant. Spectrosc. Radiat. Transfer, (60), 665 (1998).
8. Sec 53, Subpart A, Pt. 53, Vol. 40, Protection of Environment, Code of Federal Regulation. Published by the Federal Register, National Archives and Records Administration. USA.
9. App. A, Pt. 60, Vol. 40, Protection of Environment, Code of Federal Regulation. Published by the Federal Register, National Archives and Records Administration. USA.
10. Strategy for the Implementation of the Global Atmosphere Watch Programme (2001 – 2007). A Contribution to the Implementation of the WMO Long-Term Plan. No. 142. June 2001.